Available online at www.sciencedirect.com
SCIENCE DIRECT®
Journal of Molecular Catalysis A: Chemical 218 (2004) 229–239
JOURNAL OF MOLECULAR CATALYSIS A: CHEMICAL
www.elsevier.com/locate/molcata

Ni–Pt loaded silicoaluminophosphate molecular sieves for hydroisomerisation of n-heptane

I. Eswaramoorthi*, N. Lingappan

Department of Chemistry, College of Engineering, Anna University, S.P. Road, Chennai-600 025, India

Received 22 October 2003; received in revised form 9 April 2004; accepted 12 April 2004

Abstract

Silicoaluminophosphates SAPO-5 and SAPO-11 were hydrothermally synthesised and loaded with 0.2 wt.% Pt and varying (0, 0.2, 0.4 and 0.6 wt.%) amount of Ni. The line broadening XRD and TEM analyses of Ni–Pt/SAPOs indicate that the average size of Ni–Pt particles increases with increasing Ni addition. The ESCA studies reveals that complete reduction of Ni is observed only up to 0.4 wt.% Ni addition. The acidity of the catalysts analysed by TPD of ammonia revealed that added Ni species occupy the acid sites of SAPOs. Catalysts 0.4 wt.% Ni and 0.2 wt.% Pt loaded SAPOs show enhanced activity in n-heptane conversion, isomerisation selectivity and stability of the catalysts. Further, the selectivity towards the multibranched (MTB) isomers by protonated cyclopropane (PCP) intermediate formation is enhanced over the above catalysts. SAPO-5 based Ni-Pt catalysts show better activity than SAPO-11 based catalytic systems.

Keywords: Hydroisomerisation; Nickel; Platinum; Palladium; n-Heptane; SAPOs

1. Introduction

The major drawback of monofunctional acid catalyst is its less activity and selectivity in the transformations involving hydrocarbon such as hydrocracking and hydroisomerisation, which require a metal function for hydrogenation/dehydrogenation purposes. Conventionally, bifunctional catalysts comprises of noble metals like Pt, Pd, Re and Rh and acidic supports like γ-Al_2O_3, SiO_2, clays, zeolites (β, MOR, Y, ZSM-5) [1–3], silicoaluminophosphates (SAPO-5, SAPO-11 SAPO-41) [4,5] and even mesoporous materials like MCM-41 [6,7] are used for hydroisomerisation reactions to obtain high-octane gasoline. Corolleur et al. [8] reported that the specific activity of a metal for a given reaction may depend on the particle size of the metal. Because of sulphur poisoning effect of Pt, various promoter metals have been used in reforming catalysts. According to Ward [9], the property of a dispersed metal catalyst may be influenced by the addition of a second metal due to the formation of bimetallic clusters. Dowden [10] reported that the alloying of Pt with other metals generates very small ensembles of Pt atoms during reduction and giving uniform metal particles resulted in beneficial effect on catalytic performance. Further, the Pt-Re bimetallics on chlorinated alumina catalysts were found to be more stable and yielded a better quality product in naphtha reforming compared to a Pt/chlorinated alumina. The bimetallic bifunctional Pt-Ge/H-mordenite and Pt-Sn/H-mordenite catalysts were reported as potential catalysts for isomerisation of n-paraffins by Dufresne et al. [11]. Various metals such as Cu, Ga, Ni, Pd, Ge, Sn and Zn have already been used as promoter with Pt/zeolite catalysts for the isomerisation of n-paraffins [12,13].

Noble metal supported silicoaluminophosphates are found to be potential catalysts for hydroisomerisation reactions. Parlitz et al. [14] compared 0.1 wt.% Pd loaded with SAPO-11, SAPO-31, SAPO-17 and SAPO-5 for n-heptane isomerisation and reported that the catalytic activity of catalysts not only is a function of the number and acidic strength of their active sites, but also influenced by the size of pore apertures and the location of the catalytically active hydroxyl groups. Further, they reported that better activities and selectivities for high octane branched heptane isomers are achieved with SAPO-11 and SAPO-31

* Corresponding author. Tel.: +91-44-22351126; fax: +91-44-22200660.
E-mail address: eswarchem@hotmail.com (I. Eswaramoorthi).

1381-1169/$ – see front matter © 2004 Elsevier B.V. All rights reserved.
doi:10.1016/j.molcata.2004.04.007

than with SAPO-17 and SAPO-5. Sinha and Sivasanker [15,16] studied n-hexane isomerisation over Pt/SAPO-11 and Pt/SAPO-31 and reported a protonated cyclopropane (PCP) structure as intermediate. Campelo et al. [17] studied n-heptane hydroisomerisation and hydrocracking on 0.5 wt.% Pt impregnated SAPO-5 and SAPO-11 and reported that SAPO-5 acts as an excellent isomerisation catalyst at low temperatures, while at higher temperatures, no isomerisation occurred. On the other hand, SAPO-11 behaves as an excellent isomerisation catalyst over the temperature range 300–450 °C. Meriaudeau et al. [18] compared the n-octane hydroisomerisation over 0.6% Pt and 1.2% Pd loaded SAPO-11 and SAPO-41 and found very high selectivity (around 90%) towards isomerisation in all the cases. Further, they observed that grain sizes have a profound effect on conversion. Hochtl et al. [19] compared n-heptane hydroisomerisation over Pd impregnated over SAPOs and CoAPOs and found higher activity and selectivity to dibranched isomers over CoAPOs due to their higher acidity. Hochtl et al. [4] further studied hydroisomerisation of heptane isomers over 0.1–2 wt.% Pd impregnated SAPO-5 and SAPO-11 and found that at a fixed acid site concentration, the activity increased until the Pd/acid site ratio of 0.03 and concluded that the distance between acid and metal sites has only a minor effect as long as the supported metal particles and the SAPO phase were in direct contact. In our previous study [20], Ni-Pt loaded SAPO-5 and SAPO-11 catalysts were used for n-hexane hydroisomerisation and found that Ni addition up to 0.4 wt.% over 0.2 wt.% Pt increases the conversion and isomerisation and DMBs selectivity due to better metal–acid balance between catalytically active Ni–Pt particles formed and acid sites of the supports. Similar observations were made over Ni–Pt supported zeolite-β, mordenite and Y for n-hexane hydroisomerisation [21,22]. Hence, in the present study, it is proposed to study the effect of Ni addition (promoter) to Pt supported SAPO-5 and SAPO-11, which are differing in acid strength, acid site density and pore size and shape, on hydroisomerisation of n-heptane. The activity and selectivity of the catalysts are to be correlated with physico-chemical characteristics of the catalytic materials.

2. Experimental

2.1. Synthesis of SAPO-5 and SAPO-11

Silicoaluminophosphate molecular sieves SAPO-5 (AFI) and SAPO-11 (AEL) were hydrothermally synthesised using the following gel composition $0.1SiO_2$: 1TEA: $1Al_2O_3$: $1P_2O_5$: $40H_2O$ and $0.1SiO_2$: 1DPA: $1Al_2O_3$: $1P_2O_5$: $40H_2O$, respectively. In a typical synthesis, aluminium isopropoxide (20.8 g) was soaked with 30 ml of water for a day. Phosphoric acid (7.5 g) diluted with 15 ml water was added drop by drop under vigorous stirring until to get a homogeneous mixture. Tetraethylorthosilicate (1.5 ml) was added drop by drop with stirring. Then triethylamine (9.2 ml) for SAPO-5 and dipropyl amine (10.2 ml) for SAPO-11 was added drop by drop as template with stirring and stirring was continued to another 1 h. The pH of the gel was adjusted to 4–4.5 and the resultant material was transferred to 300 ml stainless steel autoclave, sealed and placed in a hot air oven maintained at 175 °C for SAPO-5 and at 200 °C for SAPO-11 for 5–6 days. At the end of crystallisation, the products were filtered, washed and dried at 120 °C for 12 h. The calcination was carried out at 550 °C for 6 h to remove the template molecules. The calcined and dried SAPO-5 was loaded with 0.1 and 0.2 wt.% Pt by incipient wetness impregnation (IWI) and the resulting catalysts are designated as A_1 and A_2, respectively. Similarly, catalysts B_1 and B_2 were obtained by impregnating 0.1 and 0.2 wt.% Pt over SAPO-11. Parts of the catalyst A_2 was impregnated with 0.2, 0.4 and 0.6 wt.% Ni by IWI and are designated as A_3, A_4 and A_5, respectively. Catalyst B_2 after impregnation with 0.2, 0.4 and 0.6 wt.% Ni resulted in catalysts B_3, B_4 and B_5, respectively. For comparison purposes, 0.2 wt.% Pt and 0.4 wt.% Pd loaded over both SAPO-5 and SAPO-11 by IWI and are designated as catalysts A_6 and B_6, respectively. Metal loadings were done with aqueous solutions of chloroplatinic acid (Sisco Research Laboratory) (2×10^{-4} g Pt per millilitre), nickel nitrate (Central Drug House) (5×10^{-4} g Ni per millilitre) and tetrammine palladium chloride (Aldrich) (2×10^{-4} g Pd per milliliter). The metal loaded catalysts were dried at 120 °C and reduced at 400 °C for 6–7 h under hydrogen flow (30 ml/min/g).

2.2. Characterisation

The purity of hydrothermally synthesised SAPO-5 and SAPO-11 was analysed using Rigaku X-ray diffractometer (XRD) with Ni filtered Cu Kα radiation ($\lambda = 1.54$ Å) in the scan range of 2θ between 5 and 60°. The line broadening XRD patterns for catalysts A_4, A_5, B_4 and B_5 were carried out using a Siefert diffractometer using Cu Kα ($\lambda = 1.54$ Å) radiation. Transmission electron microscopy measurements for the reduced Ni-Pt catalysts were carried out in JEOL 200 kV electron microscope operating at 200 kV. Specimens were enlarged using thin photographic paper. The size of all the metal particles visible in the photograph were measured manually and averaged. The state of Pt and Ni in the reduced catalysts was analysed by ESCA. The ESCA spectras were acquired with a surface analysis system (ESCALAB-MK11, VG Scientific) using the Mg Kα radiation (1253.6 eV) with pass energy of 50 eV. The total acidity of catalysts was measured by TPD of ammonia by TGA method. The detailed experimental procedures for ammonia adsorption were described in our earlier reports (20–22). The extent of ammonia adsorbed over each catalyst was measured by TGA in a TA 3000 Mettler system. Surface area measurements were carried out in Sorptomatic 1990 CE Instrument following the BET procedure using N_2 as adsorbent at liquid nitrogen temperature.

2.3. Catalytic studies

The n-heptane hydroisomerisation reaction was carried out at atmospheric pressure in a fixed bed down flow quartz reactor in the temperature range 225–375 °C in steps of 50 °C. Catalyst (1.5 g) was packed in the reactor, placed in a tubular furnace, reduced at 400 °C for 6–7 h under hydrogen flow (30 ml/min/g) and the temperature was lowered to the reaction temperature. The reactant n-heptane was fed into the reactor by a syringe pump at LHSV = 1.0 h^{-1} and pure hydrogen gas (20 ml/min/g) was passed with reactant and preheated. The reaction products were passed through condenser in ice cold condition and were collected in a trap kept in ice with a time interval of 1 h. The products were analysed by Hewlett Packard 5890A gas chromatograph equipped with FID and identified by GC–MS (SHIMADZU QP5000).

3. Results and discussion

3.1. Characterisation

3.1.1. XRD

The position and intensity of XRD patterns of SAPO-5 and SAPO-11 (not shown) are also found to be in agreement with the data given in the literature for AFI and AEL structures [14,23]. No additional peaks are observed, indicating that the samples are almost free of impurities.

3.1.2. Line broadening XRD analysis

The line broadening XRD patterns of catalysts A_4 and A_5 of A series (Fig. 1a) and B_4 and B_5 of B series (Fig. 1b) show that the intensity of the XRD peaks is found to decrease with increasing Ni addition in both the systems. By using Cu Kα X-ray, the intense peaks of Pt, Ni (cubic) and NiO (hexagonal) are expected at the 2θ values of 39.8, 44.5 and 43.3°, respectively. But in the present case, all the peaks are missing may be due to lower concentration of Pt as well as Ni species. The decrease in XRD peaks intensity with increasing Ni addition over both systems can be accounted in terms of decrease in crystallinity and increasing pore blockage of support materials by the added Pt and Ni species. The added Ni and Pt species may enter into the pores of SAPOs and grow in size during reduction step by thermal mobility of ions. The larger metallic particles formed collapses the walls of SAPOs leading to decrease in crystallinity.

3.1.3. TEM analysis

The TEM pictures of catalysts A_4, A_5, B_4 and B_5 are shown in Fig. 2a–d, respectively. The black dots seen on the support matrix are assumed to be Ni–Pt particles and the average size of them on each support is measured and presented in Table 1. The average size of the particles is found to be in nanoscale and increases with increasing Ni addition similar to our previous reports for zeolites [21]. The average particle size of catalysts A_4 and B_4 are found to be 6.35 and 6.20 nm, respectively and those of catalysts A_5 and B_5 are

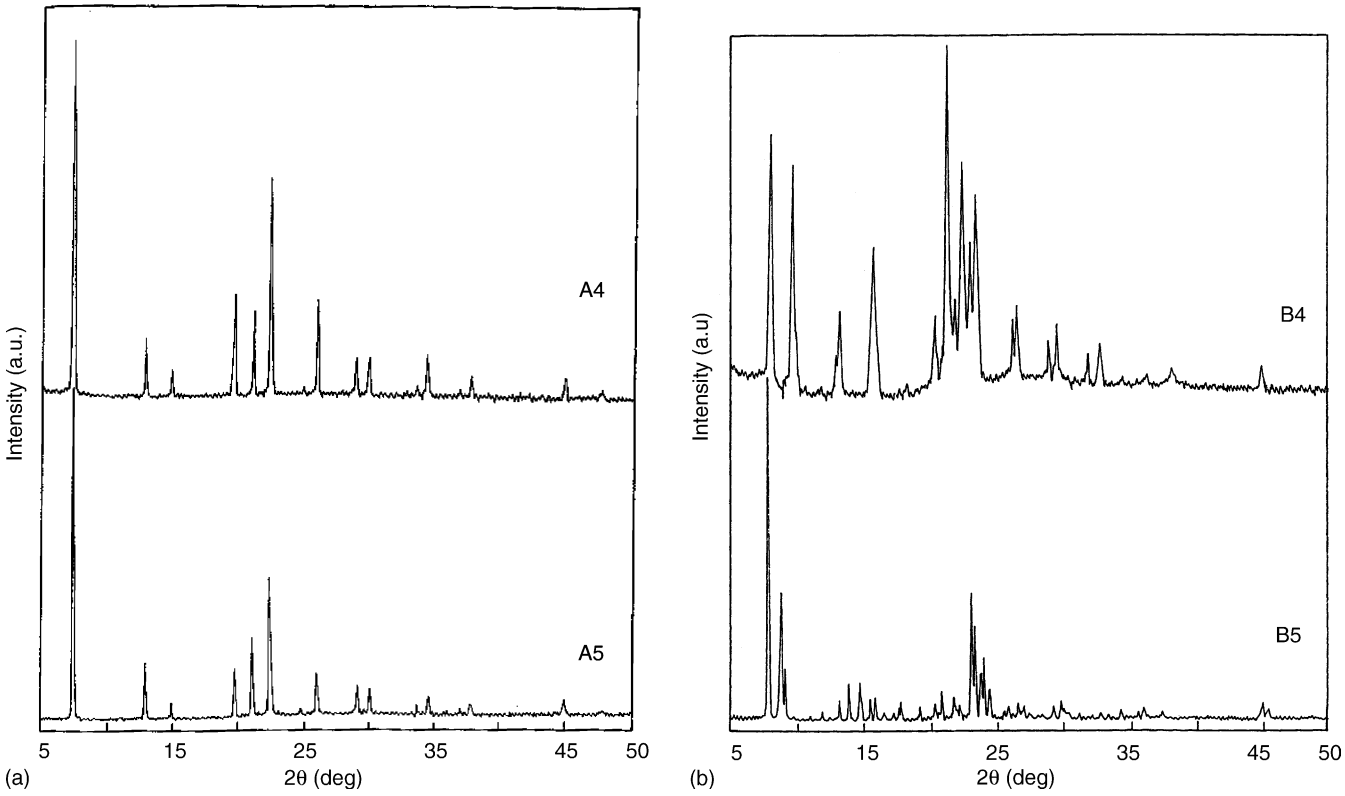

Fig. 1. Line broadening XRD patterns of (a) A_4 and A_5 and (b) B_4 and B_5.

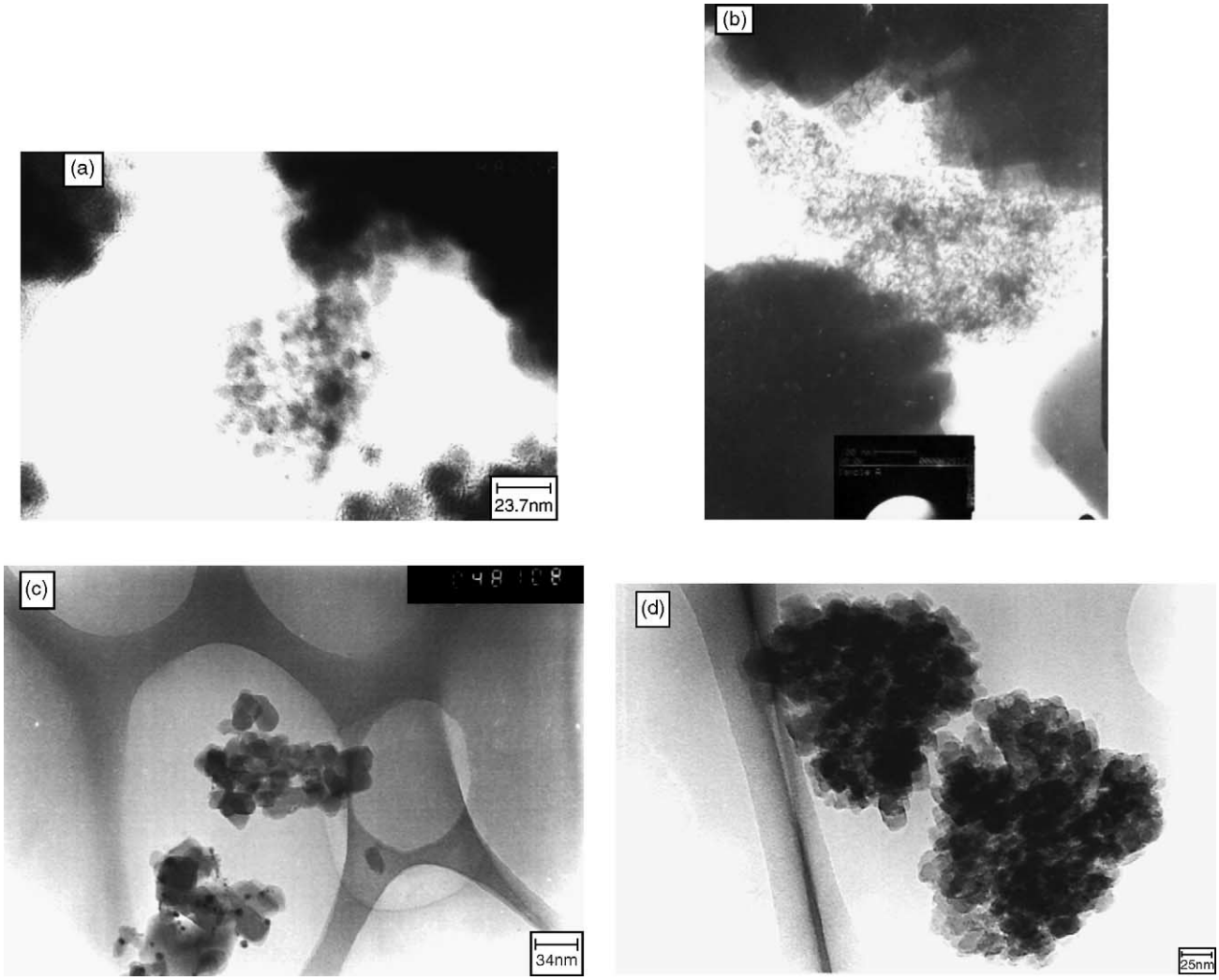

Fig. 2. TEM pictures of catalysts (a) A_4 (b) A_5 (c) B_4 (d) B_5.

Table 1
Physiochemical characteristics of A and B series catalysts

Catalyst	Pt (wt.%)	Ni (wt.%)	Surface area (m^2/g)	TPD-NH_3 mmol/g		Total acidity (mmol/g)	Particle size (nm)
				LT-peak	HT-peak		
A_1	0.1	–	–	0.478	0.260	0.738	–
A_2	0.2	–	280	0.463	0.256	0.719	–
A_3	0.2	0.2	264	0.450	0.230	0.680	–
A_4	0.2	0.4	240	0.428	0.217	0.645	6.35
A_5	0.2	0.6	228	0.405	0.195	0.600	11.38
A_6	0.2	–	245	0.435	0.207	0.642	–
A_7	–	0.6	248	0.430	0.214	0.644	–
B_1	0.1	–	–	0.408	0.224	0.632	–
B_2	0.2	–	268	0.394	0.210	0.604	–
B_3	0.2	0.2	247	0.382	0.190	0.572	–
B_4	0.2	0.4	240	0.364	0.174	0.538	6.20
B_5	0.2	0.6	236	0.345	0.150	0.495	10.42
B_6	0.2	–	225	0.365	0.182	0.547	–
B_7	–	0.6	244	0.370	0.194	0.564	–

LT, low temperature; HT, high temperature.

11.38 and 10.42 nm, respectively. Such particles may still not be smaller in size compared to the pores of SAPO-5 and SAPO-11 (Pore size of SAPO-5 and SAPO-11 are 0.73 nm (12MR) and 0.39 × 0.63 nm (10MR), respectively) with a chance for thermal mobility during reduction and hence may be located mainly outside the pores as reported by Canizares et al. [24] in Ni/H-MOR catalysts. Jao et al. [25] reported from the TPR study of (0.5) Ni- (0.26) Pt/H-MOR that a decrease in Ni reduction temperature is observed with increasing Pt concentration and presumed a catalytic reduction of Ni due to mobile platinum oxide particles colliding into each other by thermal migration and the nickel oxide particles are catalytically reduced by prereduced Pt particles. Ostard et al. [26] analysed the TEM pictures of 0.9 and 5 wt.% Pt containing MOR and found that the average Pt particle size increases with increasing Pt content as well as increasing Pt reduction temperature. Further, they reported that the catalysts reduced at higher temperature (500 °C) show twice the activity in n-heptane isomerisation than catalysts reduced at the lower temperature (350 °C) though the former catalyst with a distinctly lower Pt dispersion. Based on TEM, it is concluded that the growth of Ni–Pt particles with Ni addition is possible only the migration of Ni particles during reduction.

3.1.4. ESCA

The ESCA spectras of Pt and Ni species in reduced catalysts A_4, A_5, B_4 and B_5 are shown in Fig. 3. The Pt in the metallic state is indicated by the peaks with binding energy value around 71.2 and 74.3 eV, which are corresponding to the core level $Pt4f_{7/2}$ and $Pt4f_{5/2}$ transitions, respectively. The peak observed over catalysts A_4, A_5, B_4 and B_5 at binding energy 852.5 eV is due to the presence of nickel in metallic state. A small peak at binding energy value of 854.2 eV is observed over catalysts A_5 and B_5 and it may be due to the formation of NiO and $NiAl_2O_4$ from which the reduction of Ni^{2+} is very difficult. It is found that reduction of Ni in zeolites is difficult and multiple species of nickel are formed during reduction [27,28]. Xiao and Meng [29] analysed the reduction and oxidation behaviour of Ni containing HZSM-5 and found that many forms of nickel are exist on the surface of the zeolite due to the interaction between Ni^{2+} and zeolite. Further, they observed the surface enrichment of aluminium and nickel. But Malyala et al. [30] concluded from their XPS study on Ni/Y-zeolite and Ni-Pt/Y-zeolite catalysts that the addition of Pt causes the reduction of Ni^{2+} to Ni^0. Thus, in the present study, the added Pt (0.2 wt.%) is supposed to facilitate the reduction of nickel cations up to the range of 0.4 wt.% and above which unreduced Ni^{2+} is observed over both A and B series catalysts. Similar observations over Ni-Pt/H-β and Ni-Pt/H-MOR were already reported in our previous studies [20–22].

3.1.5. Acidity measurements

3.1.5.1. Temperature programmed desorption of ammonia. The desorption of ammonia was carried out over A and B series catalysts by TGA method. The model TPD–TGA curves for the typical catalysts A_4 and B_4 are shown in Fig. 4a and b, respectively. Table 1 depicts the temperature of desorption and amount of ammonia desorbed from each of A and B series catalysts. There are two major weight

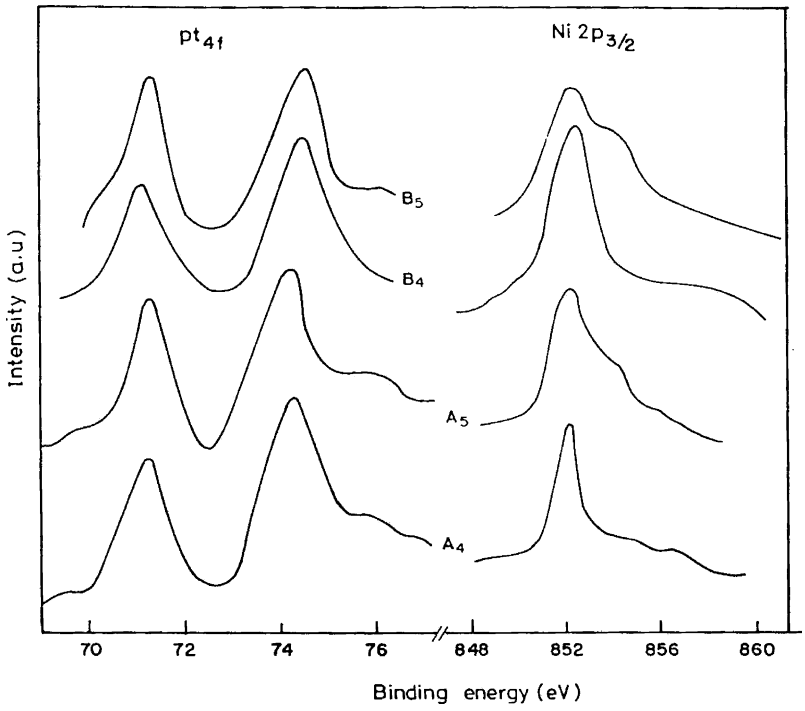

Fig. 3. ESCA spectra of catalysts A_4, A_5, B_4 and B_5.

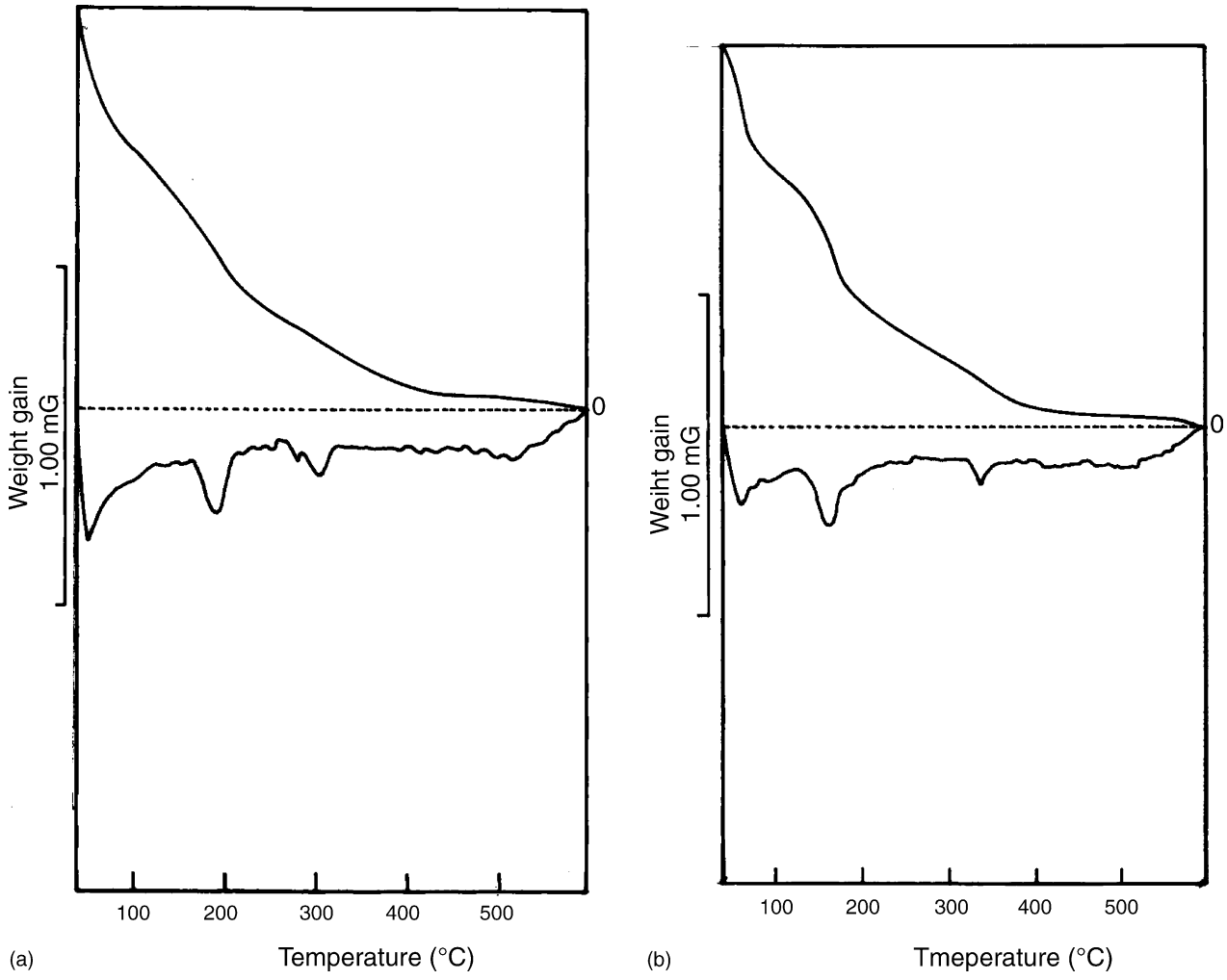

Fig. 4. TPD-TGA curves of catalyst (a) A_4; (b) B_4.

losses occurred at two different temperature ranges. The first weight loss from A and B series catalysts at the temperature region of 170–200 °C and 150–180 °C, respectively. The high temperature desorption occurs at 280–310 °C for A series and at 325–350 °C for B series catalysts. Choung and Butt [31] measured the total acidity of SAPO-11 and 2 wt.% Pd impregnated SAPO-11 by TPD of NH_3 and found that the higher temperature (330 °C) desorption peak is missing for 2 wt.% Pd/SAPO-11 and suggested that a significant number of strong acid sites are lost due to the Pd loading. Further, they considered that the lower temperature peak at 170 °C is due to the Lewis acid sites of the catalyst, while the two higher temperature peaks (240 and 330 °C) represent weak and strong Brønsted acid sites. On the basis of above result they concluded that Pd/SAPO-11 has significantly smaller number of Brønsted acid sites than unloaded SAPO-11. It is observed from Table 1, that the amount of ammonia desorbed and hence the total acidity are found to decrease with increasing Ni loading in both series catalysts. Addition of 0.4 wt.% Ni over 0.2 wt.% Pt/SAPO-5 (A_4) decreases the total acidity to 0.645 from 0.719 mmol/g and in the case of SAPO-11, same amount of Ni addition decreases the acidity to 0.538 from 0.604 mmol/g. But there is no significant change in desorption temperature is observed with increasing Ni addition indicating that the strength of acid sites is not affected by Ni addition. Also the acid strength and number of acid sites are found to be slightly higher for SAPO-5 based catalysts (A series) than SAPO-11 based (B series) catalysts. The BET surface area of A and B series catalysts are also found to be in the same trend i.e. surface area (Table 1) decrease with increasing Ni loading. The surface area values of SAPO-5 based catalysts are found to be more than that of SAPO-11 based catalysts may be due to larger pore size in SAPO-5.

3.2. Catalytic studies

Hydroisomerisation of n-heptane was carried out over A and B series catalysts in the temperature range 225–375 °C and the product distributions are presented in Tables 2 and 3, respectively. Product analysis shows that 2-methyl hexane (2MH), 3-methylhexane (3MH) 3-ethyl pentane (3EP),

Table 2
Product distribution of n-heptane hydroisomerisation over A series of catalysts

Products	225 °C							275 °C						
	A_1	A_2	A_3	A_4	A_5	A_6	A_7	A_1	A_2	A_3	A_4	A_5	A_6	A_7
2MH	6.3	9.5	10.7	13.3	13.0	14.8	7.2	9.5	12.0	14.3	15.2	14.5	16.3	8.5
3MH	5.0	8.0	9.6	11.5	10.5	11.7	5.0	7.5	9.8	12.0	13.3	12.0	14.0	6.4
3EP	–	–		–	–	–	–	–	0.5	1.0	1.5	1.0	2.0	–
23DMP	1.0	1.0	2.0	3.6	2.0	3.8	1.3	1.5	2.0	4.0	5.2	4.0	6.0	2.0
24DMP	–	0.5	1.0	2.0	1.0	2.0	1.0	1.0	1.5	2.5	3.6	2.6	4.5	1.5
22DMP	–	–	–	1.0	–	1.5	–	–	1.0	1.5	2.0	1.4	2.2	1.0
33DMP	–	–	–	–	–	1.0	–	–	–	–	1.0	1.0	1.5	–
223TMB	–	–	–	–	–	–	–	–	–	–	–	–	–	–
Cracked products	3.2	3.8	4.5	5.0	7.0	4.0	4.5	5.0	6.6	8.2	9.0	10.5	8.0	7.4
Conversion (wt.%)	15.5	22.8	27.8	36.4	33.5	38.8	19.0	24.5	33.4	43.5	50.8	47.0	54.5	26.8
2MH/3MH	1.26	1.18	1.11	1.15	1.23	1.26	1.44	1.26	1.22	1.19	1.14	1.20	1.16	1.32
2MH/23DMP	6.3	9.5	5.3	3.6	6.5	3.9	5.5	6.3	6.0	3.5	2.9	3.6	2.7	4.2
Mo/Mu	11.3	11.6	6.76	3.75	7.83	3.19	5.30	6.8	4.95	3.41	2.54	3.05	2.27	3.31
I/C	3.84	5	5.17	6.08	3.78	8.7	3.2	3.9	4.06	4.3	4.64	3.47	5.81	2.62
	325 °C							375 °C						
2MH	10.8	14.5	16.5	19.0	18.0	19.5	11.5	13.5	15.4	17.5	19.0	19.0	20.8	12.5
3MH	8.3	13.0	15.0	18.0	16.5	17.5	9.0	9.5	14.2	16.2	17.0	17.3	19.2	11.0
3EP	1.0	1.5	1.5	2.0	1.0	2.0	1.0	1.0	2.0	2.5	3.0	3.5	3.0	1.0
23DMP	2.5	3.0	4.5	6.0	5.0	7.2	3.0	3.5	4.7	6.3	7.2	6.0	8.2	3.0
24DMP	1.0	2.5	4.0	5.2	4.0	6.0	1.5	2.0	3.2	4.5	6.0	4.8	6.5	1.5
22DMP	1.0	2.0	3.0	3.5	2.8	4.3	-	1.0	3.0	3.8	4.3	3.5	5.0	1.0
33DMP	–	1.0	2.0	2.7	2.0	3.0	–	–	1.5	2.5	3.0	2.0	3.8	1.0
223TMB	–	–	–	–	–	1.0	–	–	–	1.0	2.0	0.5	2.5	–
Cracked products	8.4	9.5	11.0	11.8	14.2	10.2	10.5	10.5	12.0	13.2	14.3	15.4	11.5	13.0
Conversion (wt.%)	33.0	47.0	57.5	68.2	63.5	70.7	36.5	41.0	56.0	67.5	75.8	71.0	80.5	44.0
2MH/3MH	1.3	1.11	1.10	1.05	1.09	1.11	1.27	1.4	1.08	1.08	1.11	1.09	1.08	1.13
2MH/23DMP	4.3	4.8	3.6	3.1	3.6	2.7	3.8	4.5	3.2	2.7	2.6	3.1	2.5	4.1
Mo/Mu	4.4	3.18	2.39	2.24	2.57	1.81	4.77	3.42	2.54	2.0	1.73	2.06	1.65	3.76
I/C	2.92	3.94	4.2	4.77	3.47	5.93	2.47	2.90	3.66	4.11	4.3	3.61	6.0	2.38

Mo/Mu, monobranched/multibranched; LHSV, 1.00 h^{-1}; wt. of catalyst, 1.5 g; H_2 flow, 20 ml/min/g; time on stream, 1 h.

2,3-dimethyl pentane (23DMP), 2,4-dimethyl pentane (24DMP), 2,2- dimethyl pentane (22DMP), 3,3-dimethyl pentane (33DMP) and 2,2,3-trimethylbutane (223TMB) are major products due to the skeletal rearrangement in n-heptane. Traces of cracked, dimerised and cyclised products were also observed. The conversion (wt.%) of n-heptane over A and B series catalysts obtained at different reaction temperatures (225–375 °C) are shown in Fig. 5a and b, respectively. Generally, n-heptane conversion increases with increasing reaction temperature over all the catalytic systems. Under a fixed reaction condition, SAPO-5 (A series) based catalysts always show higher n-heptane conversion than SAPO-11 (B series) based systems even though both are having more or less similar acidic properties and surface area indicating that the pore dimension plays an important role in activity. Catalysts A_1 and B_1 (0.1 wt.% Pt) show maximum conversion of 41 and 38.5 wt.% with corresponding isomerisation selectivity of 74.3 and 77.4% at 375 °C. When increasing the Pt content by 0.1 wt.%, considerable enhancement in conversion and isomerisation selectivity are observed. Maximum conversion of 56.0 and 53.7 wt.% with corresponding isomerisation selectivity of 78.5 and 82.3% are observed over catalysts A_2 and B_2 respectively at 375 °C. The effect of Ni addition to 0.2 wt.% Pt/SAPOs on n-heptane conversion was studied by increasing the addition (0.2, 0.4 and 0.6 wt.%) of Ni and studying the n-heptane conversion at different temperatures. The introduction of 0.2 wt.% of Ni on A_2 and B_2 enhances the conversion to 67.5 and 66.3 wt.% from 56.0 and 53.7 wt.%, respectively at 375 °C. In low temperature region, the corresponding changes in conversion are high. Also, 0.2 wt.% Ni addition enhances the isomerisation selectivity from 78.5 and 82.3 (over A_2 and B_2) to 80.4 and 87.9% (over A_3 and B_3) at 375 °C. The increase in n-heptane conversion, isomerisation selectivity and suppression of cracking with increasing Ni addition is similar to the observation made by Jao et al. [25] from their study of n-heptane isomerisation over Ni Pt/H-MOR catalysts. They studied the n-heptane conversion over 0.26 wt.% Pt/H-MOR with varying Ni (0.5 and 1.5 wt.%) content and found that a maximum n-heptane conversion, with high isomerisation selectivity and simultaneous suppression of fuel gas formation over 0.5 Ni 0.26Pt/H-MOR and further increase in Ni addition (>0.5 wt.%) leads to fall in activity. Further,

Table 3
Product distribution of n-heptane hydroisomerisation over B series of catalysts

Products	225 °C							275 °C						
	B_1	B_2	B_3	B_4	B_5	B_6	B_7	B_1	B_2	B_3	B_4	B_5	B_6	B_7
2MH	7.0	10.5	13.3	16.5	15.0	16.8	8.5	9.5	14.8	17.0	17.5	16.5	17.8	9.5
3MH	5.0	6.7	8.2	11.0	10.5	13.2	5.2	7.3	11.5	13.6	14.5	14.2	15.4	6.8
3EP	–	–	–	–	–	–	–	–	–	1.0	1.5	1.0	2.0	–
23DMP	1.0	1.0	1.0	2.0	1.5	3.0	1.0	1.5	1.5	3.0	3.7	3.0	4.0	2.0
24DMP	–	–	1.0	1.5	–	1.0	–	1.0	1.0	1.5	2.2	1.8	3.0	1.5
22DMP	–	–	–	–	–	1.0	–	–	0.5	1.0	1.5	1.0	1.5	1.0
33DMP	–	–	–	–	–	–	–	–	–	0.5	0.5	–	1.0	–
223TMB	–	–	–	–	–	–	–	–	–	–	–	–	–	–
Cracked products	2.0	2.3	2.8	3.5	4.0	2.8	3.2	4.5	4.7	5.6	6.0	6.8	5.2	5.5
Conversion (wt.%)	15.0	20.5	26.3	34.5	31.0	37.8	17.9	23.8	34.0	43.2	47.4	44.3	50.0	26.3
2MH/3MH	1.4	1.56	1.62	1.5	1.42	1.27	1.63	1.3	1.28	1.25	1.2	1.16	1.15	1.39
2MH/23DMP	7.0	10.5	13.5	8.2	10.0	5.6	8.5	6.3	9.8	5.6	4.7	5.5	4.4	4.7
Mo/Mu	12.0	17.2	10.7	7.85	17.0	6.0	13.7	6.72	8.76	5.26	4.24	5.46	3.71	3.62
I/C	6.5	7.91	8.4	8.8	6.75	12.5	4.6	4.2	6.23	6.71	6.9	5.5	8.6	3.78
	325 °C							375 °C						
2MH	12.2	17.3	19.2	21.4	19.7	22.0	12.0	12.6	18.2	22.0	23.2	23.5	24.0	16.5
3MH	8.5	13.0	15.5	17.0	16.5	20.0	9.0	9.0	15.5	17.8	18.7	18.5	20.5	14.0
3EP	0.5	1.0	1.5	2.5	1.5	2.8	1.0	1.0	1.5	2.2	2.5	1.8	2.5	1.0
23DMP	2.5	3.0	4.2	5.5	5.0	5.7	2.0	3.2	3.5	5.8	6.5	5.5	7.8	3.2
24DMP	1.0	1.8	2.6	3.7	3.0	3.8	1.5	2.0	2.0	4.0	5.2	4.4	6.0	1.5
22DMP	0.5	1.5	2.3	3.0	2.5	3.5	–	1.0	2.0	3.5	4.3	3.7	5.2	1.0
33DMP	–	0.5	1.0	1.5	1.0	2.0	–	1.0	1.5	2.0	2.5	1.5	3.3	–
223TMB	–	–	–	–	–	–	–	–	–	1.0	1.0	0.5	1.5	–
Cracked products	6.0	7.0	7.5	8.4	10.0	8.5	8.2	8.7	9.5	8.0	8.8	9.0	6.8	8.5
Conversion (wt.%)	31.2	45.1	53.8	63.0	59.2	68.3	33.7	38.5	53.7	66.3	72.7	68.5	77.6	45.7
2MH/3MH	–	1.33	1.23	1.25	1.19	1.1	1.33	1.4	1.17	1.23	1.24	1.27	1.17	1.17
2MH/23DMP	4.8	5.7	4.5	3.8	3.9	3.8	6.0	3.9	5.2	3.8	3.5	4.2	3.0	5.1
Mo/Mu	–	4.6	3.58	2.98	3.27	2.98	6.2	3.13	3.91	2.74	2.4	2.88	2.1	5.5
I/C	–	5.4	6.1	6.5	4.92	7.0	3.1	3.42	4.65	7.28	7.26	6.6	10.4	4.3

Mo/Mu, monobranched/multibranched; LHSV, 1.00 h^{-1}; wt. of catalyst, 1.5 g; H_2 flow, 20 ml/min/g; time on stream, 1 h.

they attributed that the decreasing fuel gas formation with increasing Ni content in terms of increase in the metallic site/acid site (N_M/N_A) ratio when increasing the Ni content. For a catalyst with higher (N_M/N_A) ratio, the diffusion distance between the two metallic sites is shorter than in a catalyst with lower (N_M/N_A) ratio. In the present case, the initial increase in conversion with suppression of cracking by increasing addition of Ni may be due to the added Ni species may increase the total metal dispersion which leads to increase in number of active metallic sites, i.e., the metallic sites/acid sites ratio may increased towards the optimum value for isomerisation reactions due to better synergism. The initial increase in isomerisation selectivity and decrease in cracking with increasing Ni addition is due to the more availability of metallic sites in the vicinity of acid sites enabling rapid hydrogenation of the carbenium ions and desorbing them as alkanes before they undergo for cracking reactions i.e., the probability for cracking the olefinic intermediate during the migration from one metallic site to another site is less. The decreasing conversion trend with increase in cracking observed over catalysts with higher Ni content may be due to the formation of bimetallic particles of larger size and presence of unreduced Ni as evidenced by ESCA. Catalysts A_5 and B_5 have average particle sizes of 11.38 and 10.42 nm by TEM analysis. These particles may not be smaller in size compared to the pores of SAPO-5 and SAPO-11 (pore size of SAPO-5 and SAPO-11 are 0.73 nm (12MR) and 0.39 × 0.63 nm (10MR) respectively) with a chance for thermal mobility during reduction and hence may be located mainly outside the pores of SAPOs [24]. Hochtl et al. [4] studied hydroisomerisation of heptane isomers over 0.1–2 wt.% Pd impregnated SAPO-5 and SAPO-11 and found that at a fixed acid site concentration, the activity on conversion increases until the Pd/acid site ratio reaches 0.03. The Pt-Pd loaded catalysts A_6 and B_6 show higher activity (80.5 and 77.6wt.%) and isomerisation selectivity (85.7 and 91.2, respectively) than any other catalytic systems. On comparison, SAPO-5 based catalysts show higher selectivity to cracked products than SAPO-11 due to slightly higher acidic strength of former than later. The Ni only loaded catalysts A_7 and B_7 also show an increasing trend in n-heptane conversion with increasing reaction temperature even though their activity is very low. But the selectivity to cracked products is very high compared with Ni-Pt catalysts

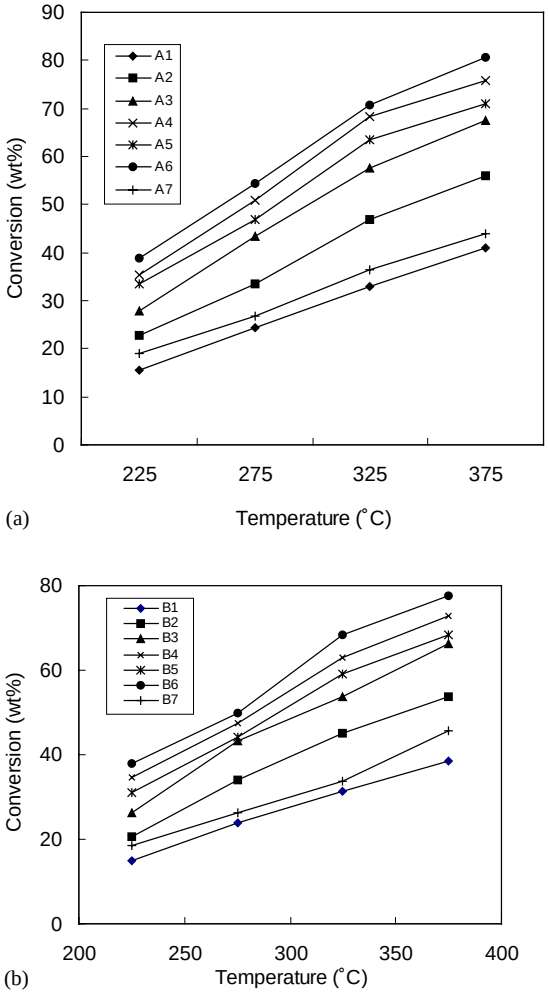

Fig. 5. n-heptane conversion over (a) A series (◆) A_1; (■) A_2; (▲) A_3; (x) A_4; (✱) A_5; (●) A_6; (+) A_7 (b) B series (◆) B_1; (■) B_2; (▲) B_3; (x) B_4; (✱) B_5; (●) B_6; (+) B_7 catalysts.

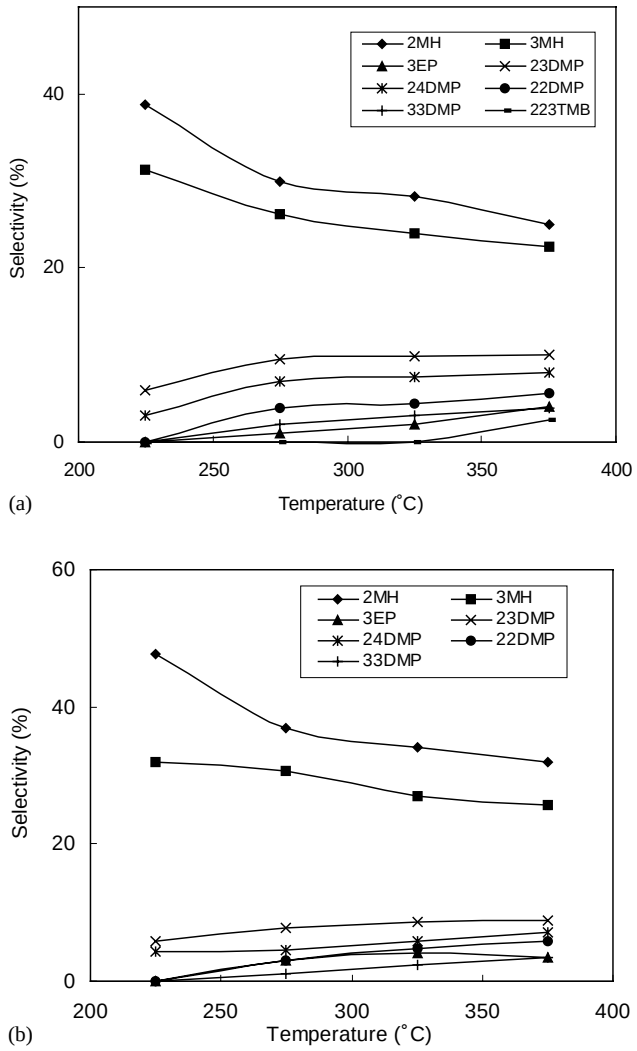

Fig. 6. Effect of temperature on the selectivity of individual heptane isomers over catalyst (a) A_4 (b) B_4.

and found to increase with reaction temperature as well as conversion.

The effect of temperature on the selectivity of individual heptane isomers over typical catalysts A_4 and B_4 is shown in Fig. 6a and b, respectively. Generally, the selectivity of the monobranched isomers 2MH and 3MH decreases with increasing temperature. The fall in selectivity of 2MH is more than that of 3MH. The selectivity of dibranched isomers 23DMP, 24DMP, 22DMP and 33DMP and tribranched isomer 223TMB is found to increase with increasing temperature. Among the dibranched isomers, the selectivities of 23DMP and 24DMP are found to be higher than other dibranched isomers (22DMP and 33DMP). Similar trend is observed over all other catalysts. The 33DMP as well as the monobranched 3EP do not appear at low (225 °C) temperature over all the catalytic systems. The increasing formation of dibranched isomers with increasing temperature as well as conversion indicates that the dibranched isomers are secondary products formed from primary monobranched isomers by protonated cyclopropane intermediate formation. The tribranched isomer 223TMB is found to appear only at higher temperatures.

The effect of temperature on the ratios among the heptane isomers over A and B series catalysts are presented in Tables 2 and 3, respectively. The thermodynamic equilibrium distribution of heptane isomers at 350 °C reported by Vazquez et al. [32] has been included in order to find the deviations of the ratios among the isomers experimentally obtained. It is observed from the Tables 2 and 3 that the monobranched/multibranched (Mo/Mu) ratio decreases with increasing reaction temperature. It is generally considered that the branching of olefins occurs through protonated cyclopropane intermediate as per the comprehensive description of carbenium ion rearrangement and cleavage by Brouwer [33]. From the point of view of PCP intermediate, the isomerisation of monobranched to dibranched heptanes goes through secondary and tertiary carbocations and therefore it should be thermodynamically favourable. But in contrast, Baltanas et al. [34] found that the rate constant for

the formation of multibranched (MTB) isomers of n-octane from monobranched (MB) is 1.5 lower than the rate of formation of monobranched isomers from n-octane. Taking into account this fact and the influence of the hydrocarbon chain length on the relative rate of formation of mono and multi branched isomers, Vazquez et al. [32] expected that in the case of n-heptane, KMu/KMo = 1/2 or KMo/KMu = 2. The Mo/Mu ratio over catalysts A_4 and B_4 are 3.75 and 1.73, 7.85 and 2.4 at 225 and 375 °C, respectively which are slightly deviated from the expected value of 2 as well as the thermodynamic equilibrium ratio of 0.62 at 350 °C. The deviation is more pronounced in SAPO-11 than SAPO-5 catalysts may be due to the more hindrance to the movement of bulky intermediates in the pores of SAPO-11 and lower acidity. The Mo/Mu ratios on SAPO-5 based catalysts were found to be lower than those over SAPO-11 based catalysts. According to Brouwer and Olederick [35] the isomersiation of methyl hexanes into dimethyl pentenes occurs through PCP mechanism. The increasing MTB formation with increasing Ni content (up to threshold values) as well as temperature indicates that the addition of Ni and high reaction temperature favour the protonated cyclopropane intermediate mechanism which is considered as one slower than 1,2 alkyl hydride shift mechanism which leads to again the formation of monobranched isomers. The enhancement of PCP mechanism over catalysts with Ni content up to the threshold values may be due to the better synergism between metal–acid sites leading to monomolecular mechanism. Catalysts with high average metal particle sizes are found to be not favouring PCP mechanism may be due to the larger particle size which affects the development of better metal–acid synergism. The unreduced Ni (shown by ESCA), which is not a active species in dehydrogenation–hydrogenation step of isomerisation has too its effect on the entire isomersiation scheme of n-heptane and hence ratio among the isomers.

The 2MH/3MH ratio over all the catalytic systems is found to decrease slightly with increase in temperature and the same trend is followed even in Ni free and Ni only loaded catalysts. The 2MH/3MH ratio is found to deviate more from the thermodynamic equilibrium ratio of 0.81. The deviation increases with increasing Ni content indicating that there is some inhibition in the formation of 3MH, formed from 2MH by the 1,2-alkyl hydride shift which is normally faster than the PCP mechanism. The decrease in Mo/Mu ratio and increase in 2MH/3MH ratio with increasing Ni content indicate that the Ni addition facilitates the multibranched isomers formation through PCP intermediate and suppresses the faster 1,2 alkyl hydride shift which usually leads to the formation of 3MH from 2MH.

According to Blomsma et al. [3], the formation of gem-dimethyl isomers (22DMP and 33DMP) is not possible by the dimerisation-cracking (bimolecular) mechanism. But in the present case, considerable amounts of 22DMP and 33DMP are formed over all the catalytic systems and found to increase with increasing reaction temperature. Hence, the n-heptane isomerisation is considered to follow the mechanism of carbenium ion rearrangement and cleavage. According to comprehensive description of rules for carbenium ion rearrangement and cleavage given by Brouwer and Oelderik [35], the carbenium ion isomerisation that leads to change in degree of branching occur through protonated cyclopropane intermediate formation. Hence, the 2MH/23DMP ratio is considered as an indication of rate of branching of heptane by protonated cyclopropane intermediate mechanism. The effect of Ni addition on the ratio of 2MH/23DMP is studied by comparing the ratios over Ni free and Ni containing catalysts at different reaction temperatures (Tables 2 and 3). It is observed that the 2MH/23DMP ratio decreases with increasing Ni addition up to 0.4 wt.% over both A and B series catalysts at all temperatures indicating the operation of PCP intermediate mechanism over catalysts with 0.4 wt.% Ni and 2 wt.% Pt.

The isomerisation/cracking (I/C) ratio of catalyst is an indication of its suitability to isomerisation reactions. A good

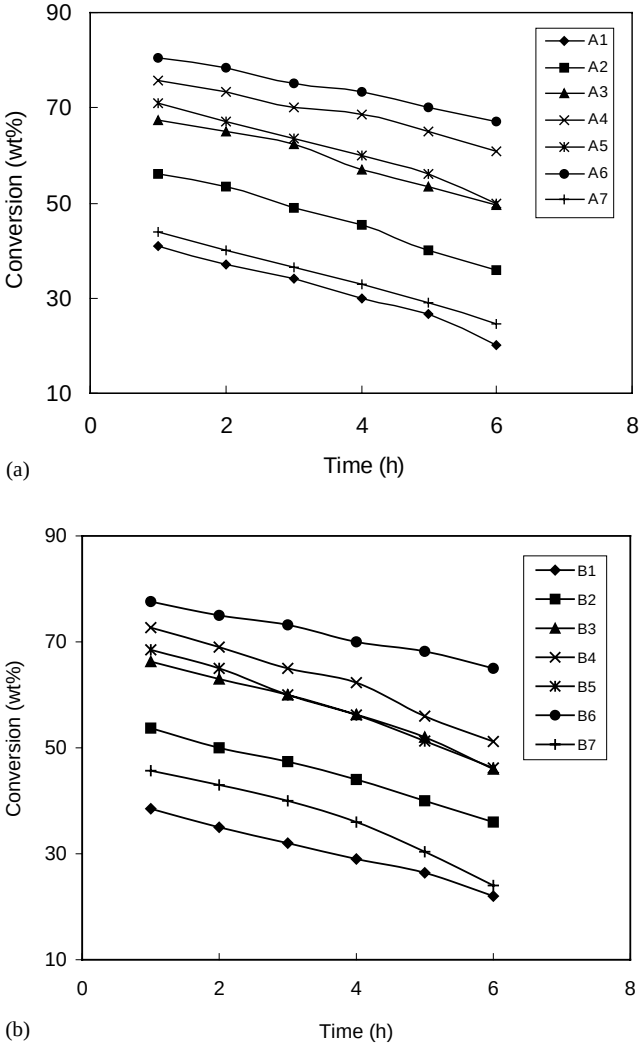

Fig. 7. Effect of time on stream on n-heptane conversion over (a) A series (b) B series Catalysts at 375 °C.

isomerisation catalyst must have very high I/C ratio. An increasing trend in I/C ratio is observed up to the Ni addition of 0.4 wt.% in both A and B series catalysts (Tables 2 and 3). Further Ni addition decreases the I/C ratio indicating the higher cracking activity of larger bimetallic particles. The I/C ratio over all the catalytic system is found to decrease with increasing temperature indicating that higher temperature favours cracking.

The sustainability of the catalysts in n-heptane hydroisomerisation reaction is studied by conducting the time on stream study for 6 h at 375 °C and the n-heptane conversions over A and B series catalysts are presented in Fig. 7a and b, respectively. All the catalysts show a fall in conversion with time. Catalysts A_4 and A_6 of A series and B_4 and B_6 of B series show the minimum fall in their activity. Catalysts without Ni (A_1 and B_1) and Ni only loaded (A_7 and B_7) show the maximum fall in activity with time. The fall in activity of the catalysts can be accounted in terms of coke formation due to cracking, which occupy the active sites of the catalyst leads to fall in activity.

4. Conclusion

The silicoaluminophosphates SAPO-5 and SAPO-11 were hydrothermally synthesised and loaded with Pt and Ni in various combinations. The line broadening XRD and TEM analysis of Ni-Pt/SAPOs indicate the average size of metal particles increases with increasing Ni addition. The ESCA study shows the existence of unreduced Ni over catalysts with higher Ni content (0.6 wt.%). The acidity measurements indicate the occupation of some of the acid sites by added Ni species. Catalysts 0.4 wt.% Ni and 0.2 wt.% Pt loaded SAPO-5 and SAPO-11 show an enhanced activity in n-heptane hydroisomerisation compared to catalysts with higher and lower Ni content. Further, the above catalysts found to enhance isomerisation selectivity, high octane DMPs selectivity through protonated cyclopropane intermediate mechanism and sustainability of the catalysts. SAPO-5 based catalysts always show better activity than SAPO-11 based catalysts.

Acknowledgements

The authors gratefully acknowledge the financial support from Department of Science and Technology (DST), New Delhi, India.

References

[1] L.-J. Leu, L.-Y. Hov, B.-C. Kang, C. Li, S.-T. Wu, T.-C. Wu, Appl. Catal. 69 (1991) 49.
[2] M. Guisnet, V. Fouche, M. Belloum, J.P. Bournonville, C. Travers, Appl. Catal. 71 (1991) 283.
[3] E. Blomsma, J.A. Martens, P.A. Jacobs, J. Catal. 165 (1997) 241.
[4] M. Hochtl, A. Jentys, H. Vinek, J. Catal. 190 (2000) 419.
[5] P. Meriandeau, V.A. Tvan, G. Sapaly, V.T. Nighiem, S.Y. Hay, L.N. Hung, C. Naccache, J. Catal. 169 (1997) 55.
[6] K. Chaudhari, T.K. Das, A.J. Chandwadkar, S. Sivasanker, J. Catal. 186 (1999) 81.
[7] M.J. Girgis, Y. Peter Tsao, Ind. Eng. Chem. Res. 35 (1996) 386.
[8] C. Corolleur, S. Corolleur, F.G. Gault, J. Catal. 24 (1972) 385.
[9] J.M. Ward, Fuel Process. Technol. 32 (1993) 55.
[10] D.A. Dowden, Catalysis, in: C. Kemball, D.A. Dowden (Eds.), vol. 2, The Chemical Society, London, 1977, p. 1.
[11] P. Dufresne, J.P. Franck, F. Raatz, C. Travers, US Pat. 4977121.
[12] J.K. Lee, H.K. Rhee, J. Catal. 177 (1998) 208.
[13] R. Le Van Mao, M.A. Saberi, Appl. Catal. A: General 199 (2000) 99.
[14] B. Parlitz, E. Schreier, H.L. Zubowa, R. Eckelt, E. Lieske, G. Lieske, R. Fricke, J. Catal. 155 (1995) 1.
[15] A.K. Sinha, S. Sivasanker, Bull. Catal. Soc. India 7 (4) (1997) 1.
[16] A.K. Sinha, S. Sivasanker, Catal. Today 49 (1999) 293.
[17] J.M. Campelo, F. Lafont, J.M. Marinas, J. Catal. 156 (1995) 11.
[18] P. Mariaudeau, V.A. Tvan, G. Sapaly, V.T. Nighiem, S.Y. Hay, L.N. Hung, C. Naccache, Catal. Today 99 (1999) 285.
[19] M. Hochtl, A. Jentys, H. Vivek, Micro. Mesopor. Mater. 31 (1999) 271.
[20] I. Eswaramoorthi, N. Lingappan, Appl. Catal. 245 (1) (2003) 119.
[21] I. Eswaramoorthi, N. Lingappan, Korean J. Chem. Eng. 20 (2) (2003) 207.
[22] I. Eswaramoorthi, N. Lingappan, Catal. Lett. 87 (3–4) (2003) 133.
[23] M.M.J. Treacy, J.B. Higgins, Collection of simulated XRD powder patterns of zeolites, fourth ed., Elsevier, Amsterdam, 2001.
[24] P. Canizares, A. De Lucas, F. Dorado, A. Duran, I. Asencio, Appl. Catal. A: General 193 (2000) 71.
[25] R.M. Jao, T.B. Lin, J.-R. Chang, J. Catal. 161 (1996) 222.
[26] D.J. Ostard, L. Kustov, K.R. Poeppelimeier, W.M.H. Sachtler, J. Catal. 133 (1992) 342.
[27] Ch. Minchev, V. Kanzirev, L. Kosova, V. Pechev, W. Grunsser, F. Schimidt, in: L.V.C. Rees (Ed.), Proceedings of the Fifth International Conference on Zeolites, Heydon, London, 1980, p. 335.
[28] S. Narayanan, Zeolites 4 (3) (1984) 231.
[29] S. Xiao, Z. Meng, J. Chem. Soc., Faraday Trans. 90 (17) (1994) 2591.
[30] R.V. Malyala, C.V. Rode, M. Arsi, S.G. Hegde, R.V. Chaudhari, Appl. Catal. A: General 193 (2000) 71.
[31] S.J. Choung, J.B. Butt, Appl. Catal. 64 (1990) 173.
[32] M.I. Vazquez, A. Escardino, A. Corma, Ind. Eng. Chem. Res. 26 (1987) 1495.
[33] D.M. Brouwer, in: R. Prins, G.C.A. Schult (Eds.), Chemistry and Chemical Engineering of Catalysis Processes, Sijithof and Noordhoff, Germantown, MD, 1980.
[34] M.H. Baltanas, H. Vansina, G.F. Froment, Ind. Eng. Chem. Prod. Res. Dev. 22 (1983) 531.
[35] D.M. Brouwer, J.M. Oelderik, Recl. Trav. Chim. Pays. Bas. 87 (1968) 721.